Instabilities and Large Structures in Reattaching Boundary Layers

Promode R. Bandyopadhyay*
NASA Langley Research Center, Hampton, Virginia 23665

The underlying premise in this work is that large structures in turbulent shear flows are not universal and similar large structures in different flows owe their origins to basically similar instabilities. The turbulent boundary-layer flow over a backward-facing step and also the reattaching transitional boundary layer behind a large spanwise rod have been studied experimentally in parallel primarily to understand the origin of the curious large structures observed in the far downstream region (after 39 step heights) of the former flowfield. Simultaneous flow visualization and hot-wire anemometry and also plain-flow visualization have been carried out. In the backward-facing step, the three-dimensional mixing layer developing after detachment persists even after reattachment. The flow does not recover fully back to a regular turbulent boundary layer even far downstream of reattachment. The turbulence-producing instability of a turbulent boundary layer continues to compete with the wall-bounded mixing layer instability, giving rise to the curious schismatic arrays of large structures.

Nomenclature

c_f = coefficient of skin friction, τ_w/q_∞
d = rod diameter
H = shape factor
h = step height
n = frequency or bin size
N = bin size
q_∞ = freestream dynamic head
Re_d = Reynolds number, $U_\infty d/\nu$
R_{12} = correlation coefficient, $\overline{[u_1(t)u_2(t+T)]}/(u_{1\text{rms}}u_{2\text{rms}})$
Re_θ = Reynolds number, $U_\infty\theta/\nu$
T = lead or lag time
t = time
U_c = convection velocity of large structure in rod experiment, $0.5U_\infty$
U_∞ = freestream velocity
U_τ = friction velocity in upstream (of step) turbulent boundary layer
u = longitudinal velocity fluctuation
x = longitudinal distance: from step or downstream edge of rod
y, z = surface normal and spanwise distances, respectively
Δx = peak to valley longitudinal spread in spanwise waviness of a vortex
δ = boundary layer thickness
θ = momentum thickness or upstream rotational/irrotational interface slope of a large structure
λ^+ = cross-stream spacing λ between longitudinal vortex pairs in upstream turbulent boundary-layer wall-layer variables, $\lambda U_\tau/\nu$
ν = kinematic viscosity
τ_w = wall-shear stress
Ω = intermittency, fraction of streamwise length the flow is turbulent in a frame

Subscripts
rms = root mean square in one large structure
1, 2, and 3 = hot wires 1, 2, or 3 in rod experiment

Superscript
overbar = time-averaged value in one large structure

Introduction

In the turbulent boundary-layer flow over a backward-facing step, far downstream of the point of reattachment, curious types of large structures appear.[1] At such far downstream distances ($39h$), one expects a regular turbulent boundary to redevelop, but it does not. This work was initiated with a desire to determine the origin of these curious large structures.

Here, it is assumed that large structures in a given flow owe their origin to instabilities specific to that flow. However, there is no formal proof of this and it comes largely from the accumulated observations of the experimentalists. On the other hand, some theoreticians have speculated on an opposing view, viz., that the large structures are universal in all turbulent flows and do not owe their origin necessarily to instabilities at all.[2] However, recent helicity measurements[3] suggest that the universal large structure proposed by some theoreticians is not justified.

Therefore, it is reasonable to assume that, in reattaching turbulent boundary layers, the turbulence production process is dominated by an instability that is different from that in a regular flatplate boundary layer. Experiments have been carried out in both reattaching transitional and turbulent boundary layers, and a feature of this work is that the large structures and the instabilities giving rise to them have been considered in close association. Two experiments are described where simultaneous-flow visualization and hot-wire anemometry and also plain-flow visualization have been carried out. In one, viz., the backward-facing step, the turbulence structure is examined in the vicinity and also far downstream of the step. In the other, the forced transition of a laminar boundary layer due to a large-diameter circular rod is studied.

Experiments

Both experiments were carried out in the Low Speed Smoke Tunnel (0.9 m × 0.9 m × 12.2 m) located in the Cambridge University Engineering Department in the mid-1970s. Isolated results from the step and the rod experiments appear in Refs. 1 and 4, respectively. The backward-facing step flow has continued to receive attention.[5-10] However, the Cambridge experiments had revealed several features of the struc-

Received Aug. 23, 1990; revision received Jan. 25, 1991; accepted for publication Feb. 12, 1991.

*Senior Research Associate, Mail Stop 170. Associate Fellow AIAA.

ture of turbulence in the backward-facing-step flows which do not seem to be well known and, therefore, it was deemed worthwhile to write a comprehensive account of them.

Figures 1 and 2 show the flow geometry in the step and the rod experiments, where the nominal freestream velocities were 1.5 and 0.9 m/s, respectively. In the step flow, a turbulent boundary layer of 120-mm thickness is negotiating a backward-facing step of height 100 mm. In the incoming boundary layer, the values of Re_θ, H, and c_f are 1170, 1.426, and 0.0042, respectively. This boundary layer is deemed normal because a clear universal log-layer exists in the mean velocity profile and the longitudinal and wall-normal turbulence distributions agree with well-known flatplate turbulent boundary-layer measurements.

In the backward-facing step experiment, the aspect ratio of the step (= span/height = 9) is close to 10. So, this has no effect on the reattachment length.[11] The expansion ratio (ratio of the vertical heights after and before the step) is 1.25. This is nearly equal to 1.0 and also has negligible effect on the reattachment length.[5] However, it is not clear if the near-unit values of δ/h and the ratio of span to separation bubble length are affecting the flow after reattachment.

Smoke-flow visualization with sectional laser lighting were carried out in the step flow and the locations of longitudinal and cross-stream visualizations are shown in Fig. 1. Simultaneous-flow visualization (150 frames/s) and hot-wire anemometry were carried out in the reattaching transitional flow and the staggered hot-wire rake configuration is shown in Fig. 2. The incoming boundary layers were seeded with smoke (vaporized kerosene) to mark the rotational fluid. Linearized single hot-wire anemometers were used. The details of how the cine film and the tape-recorded hot-wire signatures are synchronized are given in Ref. 1. The backward-facing step pictures were digitized and enhanced to highlight the small scales.

Results

Reattaching Transitional Boundary Layer

Development of Spanwise Nonuniformity

In the reattaching transitional flow experiment, a flatplate laminar boundary layer encounters a large-diameter (15.9 mm) circular rod (the ratio of the laminar boundary-layer thickness to rod diameter < 1.0) resting on and spanning the floor of the tunnel. The Reynolds number is critical (Re_d = 127–166). Vortices are shed from the rod at 12 Hz (= n) which gives a Strouhal number, nd/U_∞ of 0.2. Strobe lighting showed that the flow was periodic up to $8d$ from the downstream edge of the rod. This is close to the reattachment length in a transitional backward-facing step (Ref. 5, Fig. 2). Soon after forming, the discrete transverse vortices develop a spanwise waviness. As the waviness develops, the peaks and valleys in the first several successive vortices remain aligned (Fig. 3). In transition terminology, this is called an arrayed pattern and is characteristic of triggering due to large disturbances. It is important to note that although the transverse vortex is three-dimensional, it still lies within $8d$, the periodic flow regime.

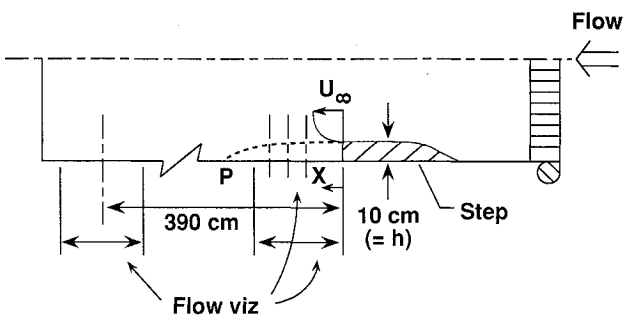

Fig. 1 Backward-facing step geometry showing locations of fully turbulent flow visualization.

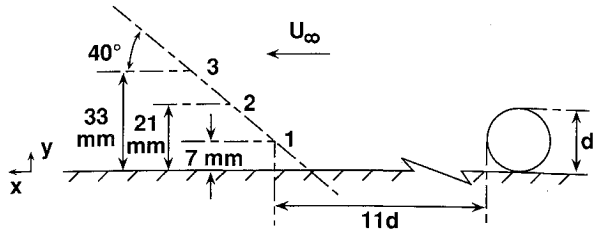

Fig. 2 Staggered hot-wire rake geometry in the transitional reattaching flow experiment.

The streamwise growth of the longitudinal spread (Δx) of the spanwise waviness of the discrete vortices is shown in Fig. 3. The growth rate varies between nonuniformities but is nearly linear in a given sample

Spreading of Vorticity Layer

Since the laminar boundary layer immediately upstream of the rod was filled with smoke, its spread immediately downstream of the rod gave an indication of the rolling and folding of the vorticity sheet. This process was studied in the movies. Figure 4 is a schematic representation of the rollups and folds of the vorticity layer obtained by superposing many frames. Note that all vorticity layers, including that attached to the wall, are interconnected. The physical significance of folding lies in the fact that it determines the decay rate of the energy spectrum. The sketch can be compared with the "threading diagram" of a Karman vortex street behind a circular rod in freestream.[12]

Disintegration of Paired Vortices

Figure 5 shows a sequence of pairing of two discrete vortices. In Fig. 5b, the vortices 1 and 2 first rotate around each other, with 1 slowing down with respect to 2, and 2 moving over 1. At the same time the cross section of 1 changes to an ellipse. This pairing in presence of the wall is similar to that observed in a plane mixing layer.[13] As the rotation of the vortex pair continues, the individual vortices become nearly indistinguishable (Fig. 5d), although no small scale is yet discernible. The vortex spacing on the upstream side of the vortices is doubled and there is a region of effectively smoke-free fluid. As shown in Fig. 5e, *the combination of the two*

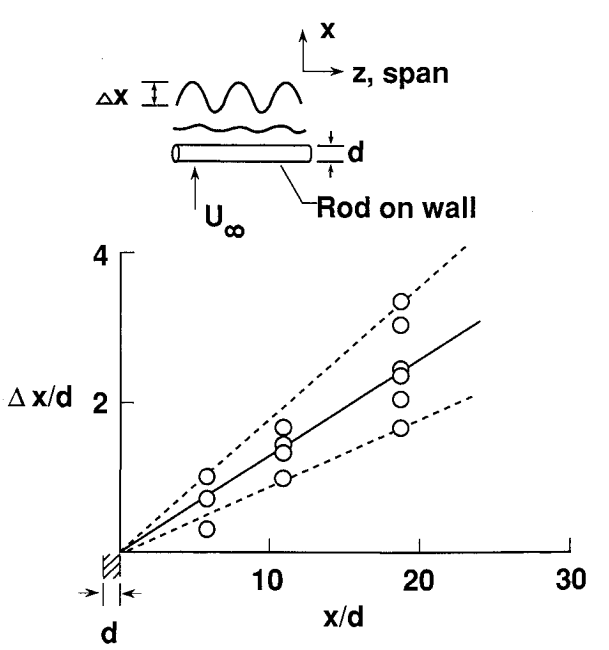

Fig. 3 Linear streamwise growth of waviness of the shed transverse vortices in the transitional rod experiment.

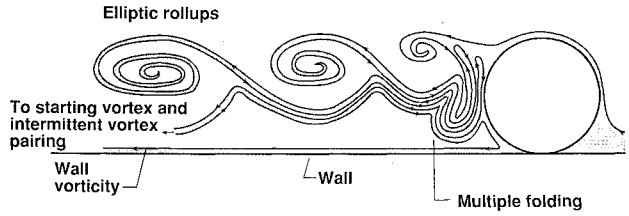

Fig. 4 Vorticity threading diagram in the transitional rod experiment.

vortices then disintegrates rather abruptly into many small scales interspersed with smoke-free fluid. (The hot-wire rake is located in this peculiar stage of the transition and it was possible to record samples of both pre- and postbreakup conditions.) The time lapse is 0.1 s both between Figs. 5b–d and 5d–e. Figure 5b–d shows that during pairing, the centroid of the pair hardly convects, but Fig. 5d, e shows that the convection velocity abruptly increases after disintegration.

The flow has also the behavior that even at $x = 17$ d, due to pairing, the large eddy doubles in height over a distance of 20 cm ($= 12.6$ d) only. This rate of growth is much higher than that in a boundary layer. This behavior is also present in the backward-facing-step experiment to be discussed later.

Phase-matched velocity signatures. Figure 6 shows the superimposed velocity signatures from individual large structures. Although, $y_3 \approx \delta$, the u_3-trace is spikey and periodic compared to what is encountered in a turbulent boundary layer. The traces are phase-matched at the marked arrows where du_3/dt is a maximum or a minimum. The large structure passage in the movies coincided with this detection. At wires 2 and 3, the traces can be divided into two groups, viz., (a, b) and (i, ii). In comparison to the former, in the latter, each large structure is characterized by a large deceleration near the phase reference location. This means a lower convection velocity in the latter group. The deceleration is preceded and followed by regions of acceleration. These distributions are similar to those in the large-scale structures in the mixing layer of a round jet where pairing takes place (Ref. 14, Fig. 12). In (i) and (ii), the reasonable phase matching means that the large structures here are inclined at about 40 deg, the inclination of the rake.

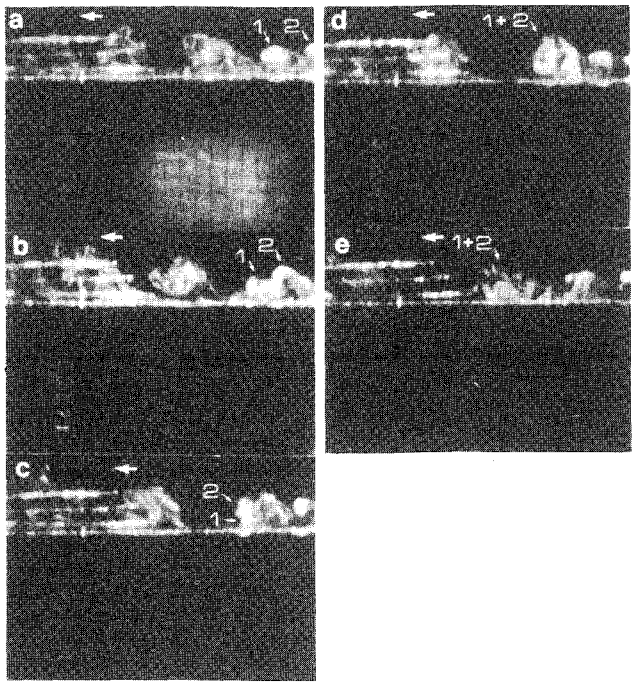

Fig. 5 Stages of pairing and breakup of large-scale structures in the reattaching transitional boundary layer.

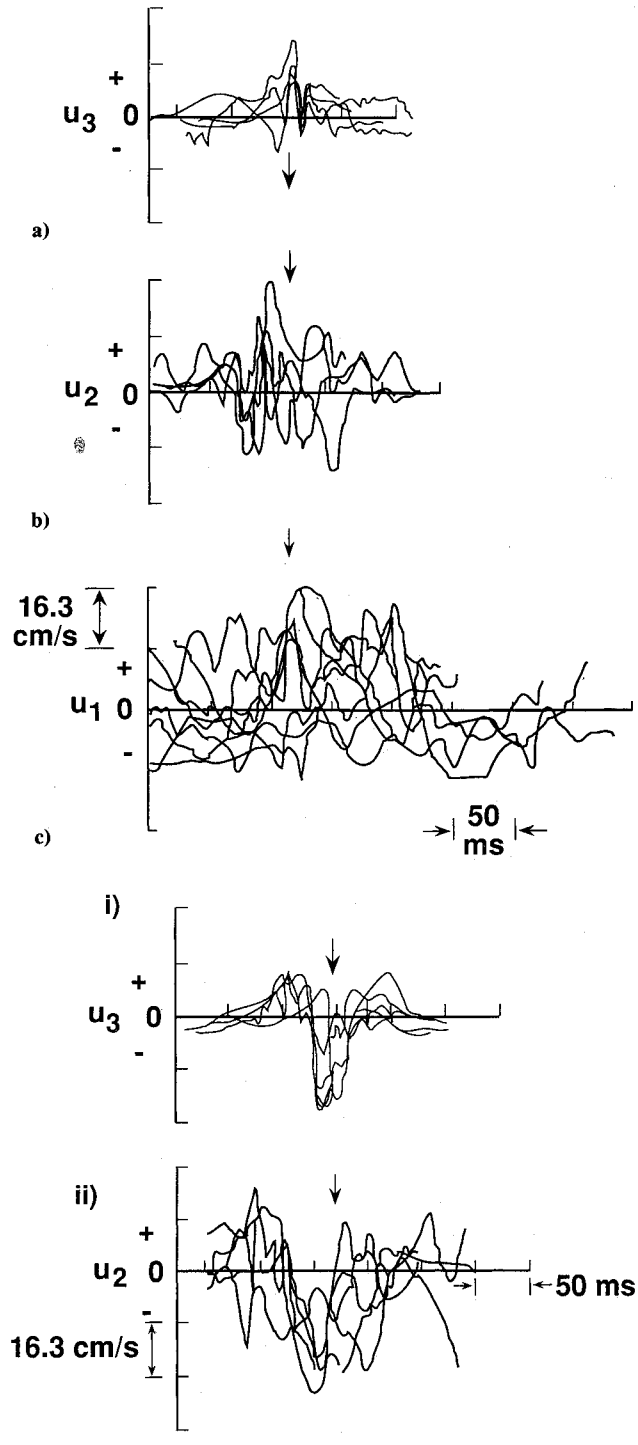

Fig. 6 Phase-aligned u-signatures in large structures in the transitional rod experiment: (i, ii), before abrupt breakup; (a–c), after abrupt breakup of the paired structures. $x_1/d = 10.82$ and $U_\infty = 0.85$ m/s.

On the other hand, the former group, viz., (a, b) is characterized by the presence of many small-scale fluctuations which lack any phase coherence and, therefore, will not survive any averaging. Also, the lack of any clear phase matching in the individual structures means that the overall structure is not inclined at 40 deg, unlike that in group (i, ii).

In many conditional averaging techniques applied to turbulent boundary-layer structure diagnostics, for example, it is reported that the individual signatures differ greatly from the ensemble-averaged one.[15] The justification for averaging

in spite of that is not clear. On the other hand, in the present work the flow visualization helped point out the existence of the pre- and postbreakup phases of the large structures, whereby the hot-wire signals could be separated into two groups in a meaningful manner.

Cross-correlations. Typical distributions of the cross-correlation coefficient R_{12} between the u-signals at the staggered wires 1 and 2 in the two types of large structures, viz., the paired and the disintegrated types are shown in Fig. 7. The wire spacing is of the order of the large scales. Near zero lead/lag times, the correlation is significant. The former has a negative correlation near zero lead/lag and this indicates the presence of an overturning motion and the latter type has a positive correlation which indicates a lack of it.

Intermittency. The distribution of Ω in the region $7.5 > x/d > 17$, that is, where the vortices pair and disintegrate, is shown in Fig. 8. In a turbulent boundary layer, $\Omega = 0.5$ is reached at $y/\delta = 0.8$. Here, this level is reached at $y/\delta = 0.5$. Also, unlike that in a turbulent boundary layer, here Ω spreads all the way to the wall. Finally, note that only five frames are adequate to obtain a stationary distribution because the flow is essentially periodic. This contrasts with the more than 100 frames that are required to get a stationary distribution in a turbulent boundary layer.

Unaveraged turbulence intensity and its flux. The distributions of the u-turbulence intensity and its streamwise flux in the individual large structures of both kinds (pre- and postdisintegration) are shown in Figs. 9 and 10, respectively. They show that the turbulence intensity in the mid-layer drops after disintegration of the paired vortices. Similarly, in the mid-layer, the negative flux is higher in the paired vortices before breakup. Before breakup, the flux distribution is closer to that in a turbulent boundary layer.[16] It is interesting that as with turbulence intensity, the flux drops (to zero) after breakup.

Turbulent Flow over a Backward Facing Step

Detached Layer

To eliminate the distraction of the structures in the incoming turbulent boundary layer or that in the recirculation region of the step and to highlight the interacting layer at a height of $y = h$, longitudinal and cross-stream visualizations were carried out immediately downstream of the step and immediately after turning the upstream smoke seeding on and also off after the supply had lasted long enough to seed the entire flow.

Longitudinal organization. Figure 11 shows several instantaneous longitudinal realizations of the smoke-marked edge of the mixing layer. The first figure displays several

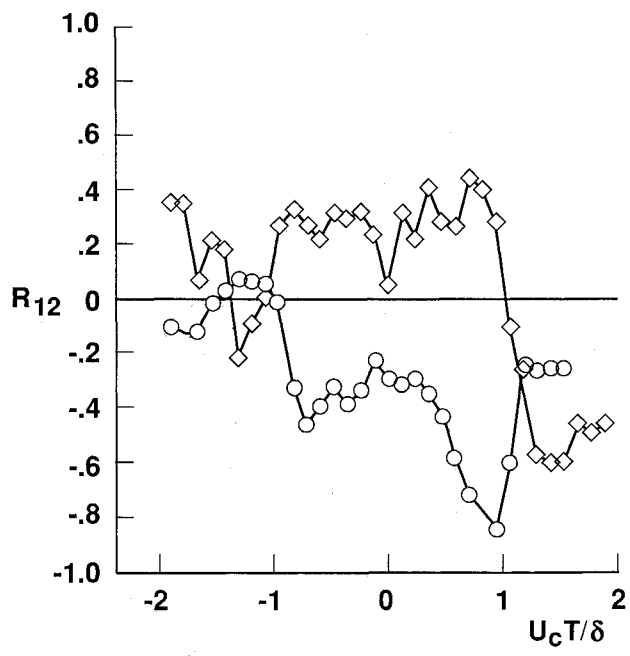

Fig. 7 Space-time correlation in individual large structures in the transitional reattaching flow ○, prebreakup; ◇, postbreakup.

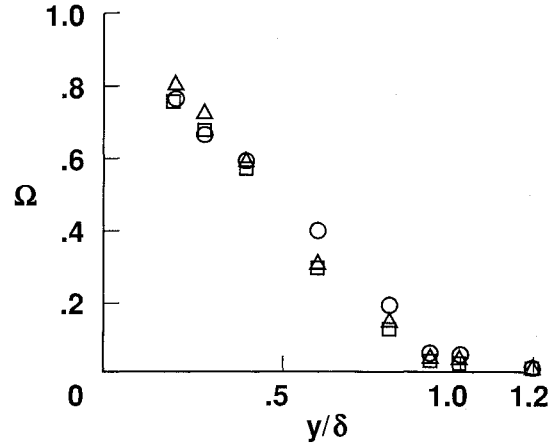

Fig. 8 Intermittency distribution in the transitional reattaching flow. Number of frames: 5 (○), 8 (△) and 12 (□).

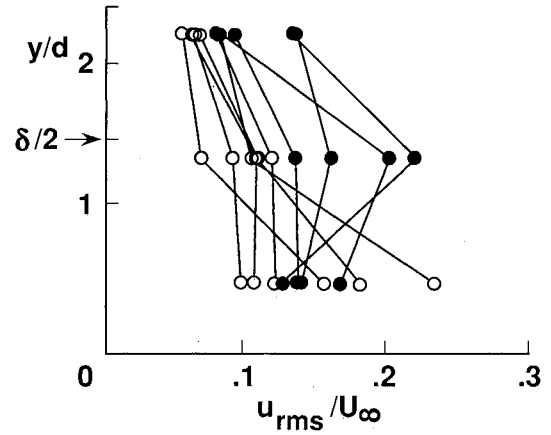

Fig. 9 Longitudinal turbulence intensity in individual large structures in the rod experiment. The ● represent the prebreakup and ○ the postbreakup conditions.

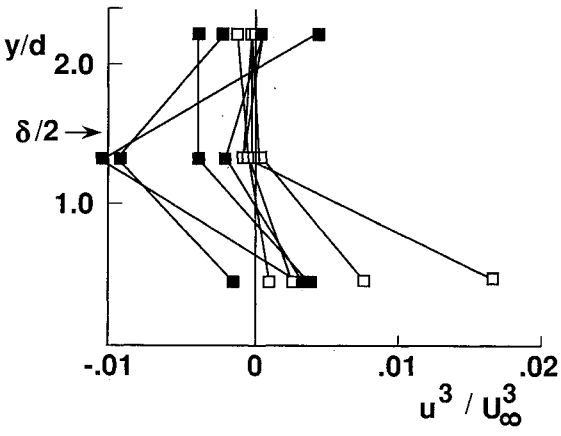

Fig. 10 Longitudinal turbulence diffusion in individual large structures in the rod experiment. The ■ represent the prebreakup structures which are boundary layer like and the □, which correspond to a depleted diffusion, represent the postbreakup structures.

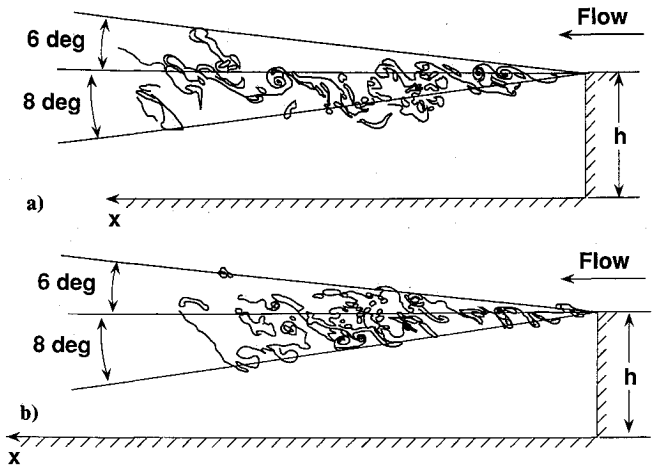

Fig. 11 Instantaneous boundary of the separated shear layer in the step flow.

concentrated vortices, but the mixing layer-like large-scale vortex structures are not obvious. However, at least up to $x/h = 3$, the layer grows linearly as in a mixing layer. The growth is slightly higher in the lower (recirculation) side. When extrapolated to the wall, the lower edge of the mixing layer reaches the surface at a distance of $6.7h$ from the step. This is close to the mean point of reattachment. (The dividing streamline is known to bend only near the point of reattachment.[5]) The passage of the large structures of the mixing layer could explain why the point of reattachment fluctuates back and forth.

Cross-stream organization. The cross-stream-flow visualization indicated that the mixing layer is three-dimensional and not two-dimensional as is commonly observed in controlled mixing layers. The most organized feature in the cross-stream plane is the presence of many longitudinal vortex pairs as shown in the top half of Fig. 12. The sample cross sections indicate that the inner induced velocity can have varying orientations probably due to the three-dimensional nature of the transverse large scales. This implies spiraling, whose effect is to enhance stretching and mixing. The cross-stream spacing between the spiral centers, λ, which is not necessarily in the z-direction, has been nondimensionalized using the length scale ν/U_τ of the turbulent boundary layer immediately before detachment. No variation in λ^+ with x was found within $0.44 \leq x/h \leq 1.22$. The histogram in Fig. 12 shows that the mean value of λ^+ is about 25. This is lower than that in low Re_θ turbulent boundary layers where λ^+ varies between 65 and 175 (Ref. 17, Fig. 12a). Clearly, the most active shear layer in the step is growing largely independent of the incoming turbulent boundary layer.

Reattached Layer Far Downstream

Intermittency. The spread of Ω across the shear layer far downstream of the step at $x/h = 39$ is shown in Fig. 13. As in the transitional reattachment case, Ω spreads almost to the wall, a very small number of frames (15) are adequate to give a stationary distribution and an Ω of 0.5 is reached earlier, viz., at an $y/\delta = 0.6$. The distribution indicates that a regular turbulent boundary layer has not yet developed and the large structures appear nearly periodically. This is in agreement with conditional LDA measurements in an open-channel backward-facing step (which simulates sand dunes in river beds), which have shown clearly the existence of quasiperiodic trains of vortices after reattachment.[18] (River engineers call this Kolk-boil vortex shedding because of the boiling-like appearance of the vortex on the free surface.)

Large structures. At $x/h = 39$, a sample of 33 large structures have been examined. The histogram of the slope of the upstream interface is shown in Fig. 14. The distribution is

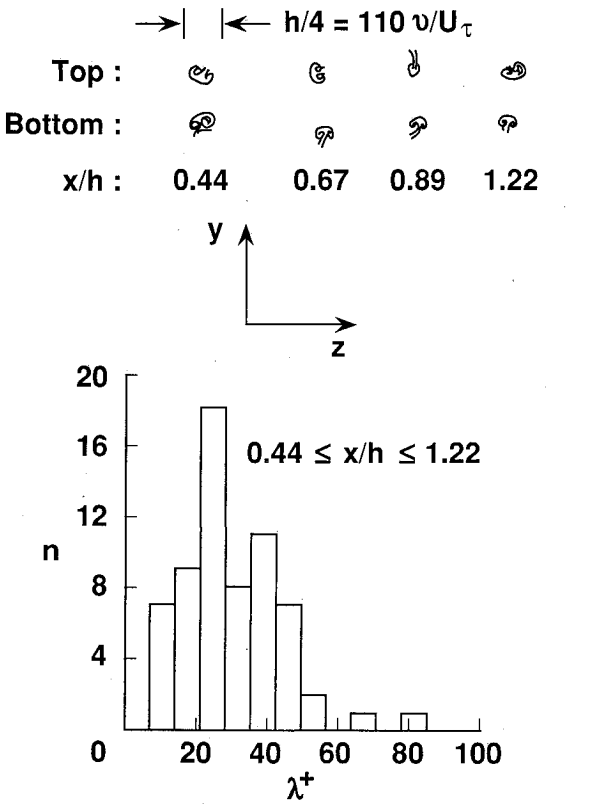

Fig. 12 Longitudinal vortex pairs and their histogram in the step flow.

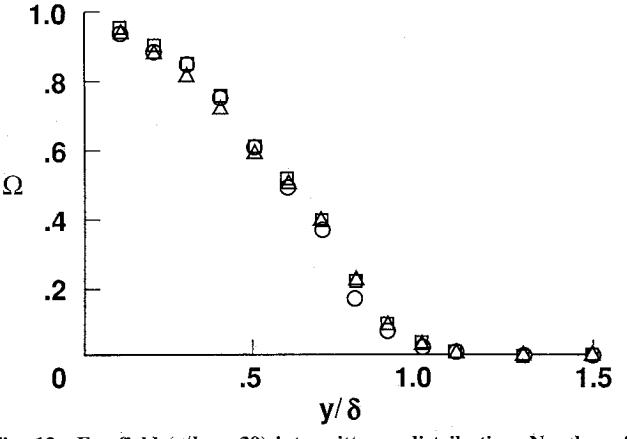

Fig. 13 Far field ($x/h = 39$) intermittency distribution. Number of frames: 15 (○), 25 (□), and 33 (△).

surprisingly spikey and the most common value is about 40 deg, and slopes greater than 40 deg are just as common as those that are less. In the reattaching transitional flow (Fig. 5, for example), the upstream interface slope lies between 40 to 60 deg. Conditional large structure measurements[9,10] show that the upstream turbulent/nonturbulent interface changes from 33 deg in the upstream flat turbulent boundary layer to 50 deg in the mixing layer at $x = 4.2h$ from the step and then on to about 60 deg at $16.8h$, well after reattachment. So, it is suspected that in the step flow at $x/h = 39$, there are some large structures which are of the regular small-slope (less than 40 deg) turbulent boundary-layer type, otherwise, the majority of the large structures in the step flow are similar to those in the reattaching transitional flow as far as the upstream interface slope is concerned.

Based on the overall morphology, it is possible to classify the large structures into three groups. Figure 15 shows an example from each group. Within each group, the structures are surprisingly similar. This probably indicates that several

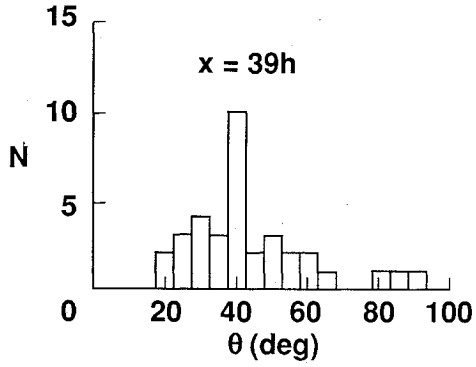

Fig. 14 Histogram of the slope of the upstream turbulent/nonturbulent interface of the large structures in the step flow after reattachment.

distinct large-scale instability modes are competing and are being observed at an early stage. The large structures with shallow ($\theta < 45$ deg) interface contain small rollups at nearly equal streamwise intervals (marked in the figure). This is an indication that an instability wave is moving upstream near the wall with respect to the freestream and there is a periodic breakdown.[4, 19] These small rollups can be called "no-slip" rollups. The streamwise extent of a spiral is about 0.05δ. However, in the group where $\theta \approx 45$ deg, there is no traveling instability wave and we suspect that a paired vortex after achieving a maximum stretching is disintegrating all over simultaneously. The third remaining large-structure group contains trains of nearly equispaced rollups where the orientation of the trains is not inclined to the wall, but is parallel to the freestream. This suggests that a wall-layer moving instability wave is not behind their formation and they have been termed "free-slip" rollups.

Discussion

An important but poorly understood feature of the reattaching flows has been the rapid decrease of the Reynolds stresses approximately downstream from the reattachment point.[5] This has been reported in both the LDA and hot-wire measurements up to $17h$ from the step.[7, 9] The stabilizing effect of convex curvature acts only very near the point of reattachment and cannot explain the continuing drop downstream. It has been argued[20] that the large eddies are torn into two in the reattachment zone and the rapid reduction in length scale is responsible for the decrease in the turbulence levels. However, the review in Ref. 5 has concluded that "the majority of the workers have disagreed that eddies are torn in two, and measurements far downstream of reattachment indicate that the free-shear-layer structure persists in the outer part of the boundary layer." The present work, on the other hand, reconciles these seemingly opposing views. It shows that the reduction in stresses is attributable to the sudden appearance of the small scales after disintegration of the paired eddies, while the free-shear-layer type of development is persisting although the flow is wall bounded.

It is possible to clarify another unexplained feature noted in the review in Ref. 5. The measurements in Refs. 21 and 22 show that immediately downstream of reattachment, Ω is less than unity near the wall. It was speculated that the eddies are alternately moving up and downstream. However, since that time no evidence has appeared that supports the alternate direction-splitting of the eddies. The present work suggests that Ω spreads almost to the wall because most of the large eddies convecting over the wall are mixing layer like, whose spacing is of the order of their height, and the wall does not play any important role in their formation.

It is interesting to note that the abrupt disintegration into smaller scales after pairing observed here in the reattaching flow does not take place after pairing in low-disturbance mixing layers where the dominant large structures are two-dimensional (for example, see Ref. 13). In spite of the many mixing-layer-like characteristics of the step, this is one aspect at variance after all, and it is attributable to the induced effect of the wall. It is suspected that the disintegration is due to a three-dimensional instability of the two intertwinning horseshoe vortices in the reattaching flow and that is why it *succeeds* the pairing instability.

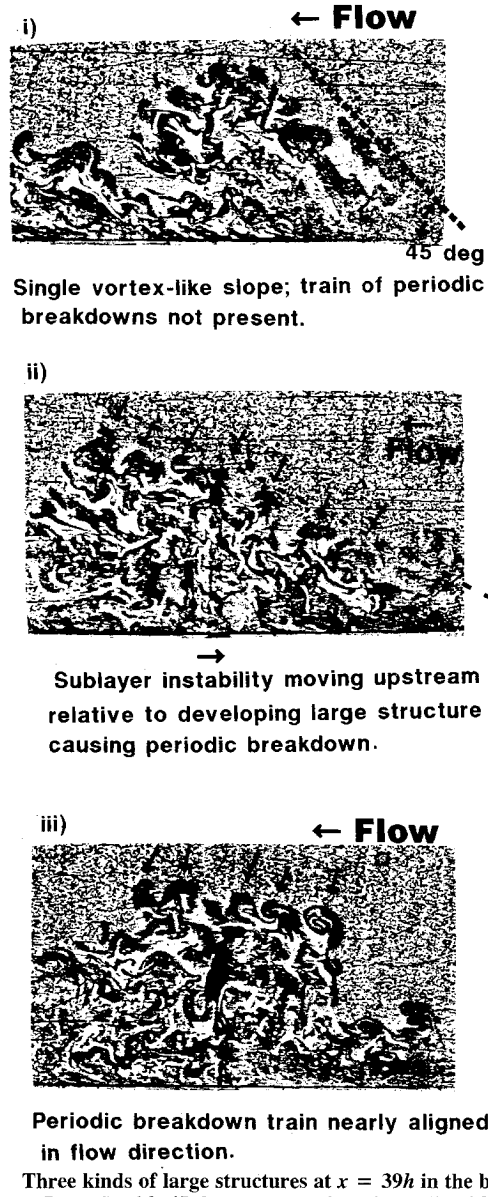

Fig. 15 Three kinds of large structures at $x = 39h$ in the backward-facing step flow: i) with 45-deg upstream interface; ii) with trains of no-slip rollups; and iii) with trains of free-slip rollups.

It is necessary to clarify the difference between this three-dimensional instability and the secondary three-dimensional instability of the two-dimensional vortical structures of a plane mixing layer.[23, 24] In the latter, pairing inhibits three-dimensionalization, whereas in the former, pairing precedes the appearance of the three-dimensional small scales. Also, in the latter, "ribs" connect the primary spanwise vortices, whereas in the former, the new spanwise vortex itself is composed of the small scales. In other words, the longitudinal scale of the ribs in the latter is much larger than that of the small scales in the latter.

The overturning motion of a large structure is an important aspect to compare between flatplate boundary layers and reattaching flows. The rod flow showed that doubling of the large-structure scale can continue even at a distance of $17h$ from the rod. Since this is caused by pairing, a strong overturning is implied. Similarly in a backward-facing step at a distance of $9.7h$ from the step, two-point correlation measurements

show that the entire boundary layer is characterized by an overturning motion.[25] Recent measurements[9] of velocity vectors in the conditionally sampled large structures also show the presence of a structure-wide overturning motion up to a distance of $16.8h$, the last measurement station. In Ref. 9, the authors have interpreted the large structure as a horse shoe vortex. In the reattaching transitional flow shown in Fig. 5, the overturning rate involved in the pairing process is much stronger than that in the large structure of a turbulent boundary layer at a similar Reynolds number.[4]

Conclusions

Experiments have been carried out to investigate the origin of the large structures in reattaching boundary layers. Two flows are examined. The first is the reattaching transitional boundary layer that develops downstream of a large spanwise rod over which a thin laminar boundary layer is passing. In the second, a turbulent boundary layer negotiates a backward-facing step. The following conclusions are drawn in the backward-facing step flow:

1) A mixing layer develops along the step after detachment. However, unlike that in most controlled mixing layer experiments, the transverse vortices in this step-flow mixing layer are not generally well identifiable and are three-dimensional. In comparison to that in the incoming turbulent boundary layer, the mixing layer contains longitudinal vortex pairs along the span whose spacing is much narrower (about one-third to one-fourth).

2) Far downstream of reattachment ($x/h = 39$), the flow exhibits the following differences from regular turbulent boundary layers. 1) The intermittency spreads almost to the wall. 2) The boundary layer growth is much larger. 3) The upstream interface of the large structures is larger than that in an undisturbed zero pressure gradient flatplate turbulent boundary layer. 4) The outer regions of the large structures contain trains of both no-slip and free-slip type small rolled-up vortices and their number abounds compared to that in both mixing layers and regular boundary layers.

The following conclusions are drawn in the transitional reattaching flow:

1) Soon after detachment, the laminar boundary layer rolls into discrete vortices whose spanwise waviness initially grows linearly with streamwise distance.

2) The flow involves a vortex core instability. In spite of the wall-bounded nature, frequently, two consecutive vortices go through a mixing-layer-type pairing process. However, unlike that in mixing layers, after pairing, the vortices disintegrate into many small scales.

3) Before breakup of the paired vortices, the structure displays an overturning motion and in the mid-layer, the u-turbulence and its longitudinal flux in each large structure are similar to that in fully turbulent boundary layers. However, after breakup, the structure does not overturn significantly, its convection velocity increases, and both the turbulence intensity and its flux drop.

The backward-facing step turbulent flow bears several key similarities to the reattaching transitional flow. It is suggested that after reattachment, the backward-facing step flow also undergoes a pairing instability and the paired vortices disintegrate into many vigorous small eddies. Experiments are needed to examine the step flow between the point of reattachment and the downstream location of $x/h = 39$ to verify this.

References

[1]Bandyopadhyay, P., "Combined Flow Visualisation and Hot-Wire Anemometry in Turbulent Boundary Layers," In *Structures and Mechanism of Turbulence I*, edited by H. Fiedler, Lecture Notes in Physics, Springer, New York, Vol. 75, 1977, pp. 205–216.

[2]Levich, E., and Tsinober, A., "On the Role of Helical Structures and 3-Dimensional Turbulent Flow," *Physics Letters A*, Vol. 93A, No. 6, 1983, p. 293.

[3]Wallace, J. M., and Balint, J. L., "An Experimental Study of Helicity and Related Properties in Turbulent Flows," *Proceedings of the IUTAM Symposium: Topological Fluid Mechanics*, edited by H. K. Moffatt, Cambridge, England, UK, 1989, 13 p.

[4]Head, M. R., and Bandyopadhyay, P., "Combined Flow Visualization and Hot-Wire Measurements in Turbulent Boundary Layers," In *Proceedings of the Workshop on Coherent Structure of Turbulent Boundary Layers*, edited by C. R. Smith and D. E. Abbott, Lehigh Univ., 1979, 98–129.

[5]Eaton, J. K., and Johnston, J. P., "A Review of Research on Subsonic Turbulent Flow Reattachment," *AIAA Journal*, Vol. 19, 1981, pp. 1093–1100.

[6]Pronchik, S., and Kline, S., "An Experimental Investigation of the Structure of a Turbulent Reattaching Flow Behind a Backward-Facing Step," 1984 Report, MD-42, Thermo. Divn., Stanford Univ., Stanford, CA.

[7]Driver, D. M., and Seegmiller, H. L., "Features of a Reattaching Turbulent Shear Layer in Divergent Channel Flow," *AIAA Journal*, Vol. 23, 1985, pp. 163–171.

[8]Adams, E. W., and Johnston, J. P., "Effects of the Separating Shear Layer on the Reattachment Flow Structure: Part 2. Reattachment Length and Wall Shear Stress," *Experiments in Fluids*, Vol. 6, 1988, pp. 493–499.

[9]Jovic, S., and Browne, L. W. B., "Evolution of Coherent Structures in the Reattachment Region of a Separated Flow," In *Proceedings of the Tenth Australasian Fluid Mechanics Conference*, Univ. of Melbourne, Australia, Dec. 11–15, 1989, Paper 8D-1, 1989, pp. 8.31–8.34.

[10]Jovic, S., and Browne, L. W. B., "Coherent Structures in a Boundary Layer and Shear Layer of a Turbulent Backward-Facing Step Flow," In *Proceedings of the Seventh Symposium of Turbulent Shear Flows*, Stanford Univ., Stanford, CA, Aug. 21–23, 1989, 24.3.1–24.3.6.

[11]de Brederode, V., and Bradshaw, P., "Three-Dimensional Flow in Nominally Two-Dimensional Separation Bubbles: I. Flow Behind a Rearward Facing Step," Imperial College Aeronautics Rept., 72-19, 1972.

[12]Perry, A. E., Chong, M. S., and Lim, T. T., "The Vortex-Shedding Process Behind Two-Dimensional Bluff Bodies," *Journal of Fluid Mechanics*, Vol. 116, 1982, pp. 77–90.

[13]Winant, C. D., and Browand, F. K., "Vortex Pairing: the Mechanism of Turbulent Mixing-Layer Growth at Moderate Reynolds Number," *Journal of Fluid Mechanics*, Vol. 63, 1974, pp. 237–255.

[14]Yule, A. J., "Large-Scale Structure in the Mixing Layer of a Round Jet," *Journal of Fluid Mechanics*, Vol. 89, 1978, pp. 413–432.

[15]Antonia, R. A., and Bisset, D. K., "Spanwise Structure in the Near-Wall Region of a Turbulent Boundary Layer," *Journal of Fluid Mechanics*, Vol. 210, 1990, pp. 437–458.

[16]Bandyopadhyay, P. R., and Watson, R. D., "Structure of Rough Wall Turbulent Boundary Layers," *Physics of Fluids*, Vol. 31, 1988, pp. 1877–1883.

[17]Kline, S. J., Reynolds, W. C., Schraub, F. A. and Runstadler, P. W., "The Structure of Turbulent Boundary Layers," *Journal of Fluid Mechanics*, Vol. 30, 1967, pp. 741–773.

[18]Nezu, I., and Nakagawa, H., "Turbulent Structure of Backward-Facing Step Flow and Coherent Vortex Shedding from Reattachment in Open Channel Flows," *Proceedings of the Turbulent Shear Flows 6*, Sept. 7–9, 1987, Toulouse, France 19-1-1, Springer, New York.

[19]Bandyopadhyay, P., "Large Structure with a Characteristic Upstream Interface in Turbulent Boundary Layers," *Physics of Fluids*, Vol. 23, 1980, pp. 2326–2327.

[20]Bradshaw, P., and Wong, F. Y. F., "The Reattachment and Relaxation of a Turbulent Shear Layer," *Journal of Fluid Mechanics*, Vol. 52, 1972, pp. 113–135.

[21]Kim, J., Kline, S. J., and Johnston, J. P., "Investigation of Separation and Reattachment of a Turbulent Shear Layer: Flow Over a Backward Facing Step," 1978 Rept., MD-37, Thermo. Divn., Stanford Univ., Stanford, CA.

[22]Chandrasuda, C., "A Reattaching Turbulent Shear Layer in Incompressible Flow," Ph.D. Thesis, 1975, Imperial College, London.

[23]Metcalfe, R. W., Orszag, S. A., Brachet, M. E., Menon, S., and Riley, J. J., "Secondary Instability of a Temporally Growing Mixing Layer," *Journal of Fluid Mechanics*, Vol. 184, 1987, pp. 207–243.

[24]Rogers, M. M., and Moser, R. D., "Development of 3-Dimensional Temporally-Evolving Mixing Layers," Symposium of Turbulent Shear Flow, 7th, Vol. 1, Stanford Univ., Stanford, CA, Aug. 21–23, 1989, pp. 9.3.1–9.3.6.

[25]Driver, D. M., Seegmiller, H. L., and Marvin, J. G., "Time-Dependent Behavior of a Reattaching Shear Layer," *AIAA Journal*, Vol. 25, 1987, pp. 914–919.